Electron interferometry: Interferences between two electrons and a precision method of measuring decoherence

Franz Hasselbach, Harald Kiesel, and Peter Sonnentag

Institut für Angewandte Physik, Universität Tübingen,
Auf der Morgenstelle 10, D-72076 Tübingen, Germany

ABSTRACT. Louis de Broglie's discovery of the wave nature of matter 80 years ago and the subsequent development of quantum mechanics by Erwin Schrödinger, Werner Heisenberg and Paul Dirac solved many riddles of those days and determined physics of the whole 20th century. Yet, after this long time, matter wave interferometry is as up to date as it was in 1927 when Louis de Broglie's hypothesis was verified, e.g., by Davisson and Germer. Atom interferometry, ion interferometry and Bose-Einstein condensates are today's fascinating applications based on de Broglie's discovery. The focus of the present contribution are Hanbury Brown-Twiss anti-correlations (i.e. interferences between two fermions (electrons)) and the quantitative observation of decoherence by electron biprism interferometry.

P.A.C.S.: 03.75.-b; 05.30.Fk; 03.65.Yz

1 Observation of Hanbury Brown-Twiss anticorrelations in a beam of free electrons

The astronomers R. Hanbury Brown and R.Q. Twiss (HBT) were the first to observe in 1956 that the fluctuations in the counting rate of photons originating from uncorrelated point sources become, within the coherently illuminated area, slightly enhanced compared to a random sequence of classical particles [1, 2, 3]. This at a first glance mysterious formation of correlations in the process of propagation turns out to be a consequence of quantum interference between two indistinguishable photons and Bose-Einstein statistics. The latter requires that the composite wave function is a symmetrized superposition of the two possible paths. For fermions, by virtue of the Pauli principle, no two particles are allowed

to be in the same quantum state. The corresponding antisymmetrized two-particle wave function excludes overlapping wave trains, i.e., simultaneous arrivals of two fermions at contiguous, coherently illuminated detectors are forbidden. These anticorrelations have been observed [4] for a beam of *free* electrons in spite of the low mean number (degeneracy) of $\sim 10^{-4}$ electrons per cell in phase space. With respect to the low degeneracy, our experiment is the fermionic twin of HBT's experiment with photons.

Correlations between successive detections of bosons resp. fermions are observed even if the emission of the two particles cannot physically influence one another because, e.g., the emission sites $\mathbf{r}_1$,t_1 and $\mathbf{r}_2$,t_2 have a space-like separation. In such a radiation field correlation builds up in the process of propagation. At points sufficienly far from the sources the field becomes, within the coherently illuminated area, highly correlated. This obervation of HBT in 1956 seemed so strange to a considerable portion of the physics community that they declared it as physically absurd[1], although the van Cittert-Zernike theorem of partial coherence which expresses the field correlations (coherence) at two points in an optical field emerging from incoherent planar sources was formulated nearly two decades before.

In the course of the very controversial discussion a physically clear, vivid explanation of these correlations, which correspond to a larger (smaller) noise in a beam of bosons (fermions) compared to a beam of classical Boltzmann particles was given by E. Purcell. In his paper [6] he writes:

'If one insists on representing photons by wave packets and demands an explanation in those terms of the extra fluctuation, such an explanation can be given. But I shall have to use language which ought, as a rule, to be used warily. Think, then, of a stream of wave packets, each about $c/\Delta\nu$ long, in a random sequence. There is a certain probability that two such trains accidentally overlap. When this occurs they interfere and one may find (to speak rather loosely) four photons, or none, or something in between as a result. It is proper to speak of interference in this situation because the conditions of the experiment are just such as will ensure that these photons are in the same quantum state. To such interference one may ascribe the "abnormal" density fluctuations in any assemblage of bosons'.

In this picture sometimes the interfering photons seem to annihilate one

[1] A lively description of the situation at that time is given in [5].

another, sometimes they seem to generate four photons. At a first glance this contradicts conservation of photon number and conservation of energy. Considering constructive interference, two photons cannot become four photons. The explanation of this paradox is that, by interference, the interval of time between two consecutive photons becomes so much smaller that the *mean photon current* corresponds to the emission of four photons within a correspondingly shorter time interval. Destructive interference, according to conservation of energy, cannot mean annihilation of the photons. In this case the two photons are forced further apart from each other into two adjacent cells in phase space. Both interference effects add up and result in an increased noise level in a beam of photons (bosons) compared to a beam of classical (Boltzmann) particles. Due to these increased fluctuations in intensity, the HBT effect is also well known as intensity interferometry.

On the other hand, the correlations of electrons in the present experiment, or more generally of any fermionic system, (antibunching) are fundamentally different from the correlations in a bosonic beam (bunching). By virtue of the Pauli principle, for fermions more than one particle in one quantum mechanical state is forbidden. In the parlance of interference this is equivalent to the fact that destructive interference is the only choice for fermions. Consequently, within the area coherently illuminated by an electron emitter electrons are only allowed to arrive one after another with a minimum distance (in time) of at least one coherence length (time). As a consequence of this behaviour the noise in a fermionic beam is smaller compared to a classical beam of particles and decreases with increasing current density (occupation of the quantum mechanically available states). It vanishes when all available states are occupied by one single fermion. As a further consequence an upper limit of the current density exists in fermionic beams.

From another point of view, HBT have shown that measuring field correlations (2nd order coherence) provides a second — apart from observing interference fringes — sometimes more handy and/or *powerful method for measuring the absolute value of the degree of coherence*. E.g., with their stellar *intensity* interferometer HBT were able to measure the diameter of Sirius, undisturbed by fluctuations of the refractive index of the atmosphere [7].

The reason why (anti)correlations between *free* photons (electrons) in coherent beams are so difficult to observe and why the fundamentally different behaviour of free bosons and fermions does not at all become

obvious in light and electron optics — in spite of the extreme difference between Bose-Einstein and Fermi-Dirac statistics[2] — is due to the very low occupation numbers (degeneracy) in phase space. Only recently, with the advent of high brightness field electron emitters with degeneracies reaching 10^{-4} an experiment for free fermions seemed to become feasible [8, 9]. The first fermionic HBT experiments in semiconductor devices where *highly degenerate* beams of electrons are conveniently available [10, 11] have been successfully performed in 1999.

1.1 Experimental procedure

The coincidence method chosen in the present 'antibunching' experiment is an alternative to HBT's correlation procedure for gathering information about correlations in a stream of particles: Two detectors are coherently illuminated by an electron field emitter. According to the Pauli principle no two electrons are allowed to be in the same quantum state, i.e., to arrive at both detectors simultaneously[3]. In other words, if our detectors had a time resolution corresponding to the coherence time T_c which is on the order of $10^{-14}\,\mathrm{s}$, no coincidences would be observed. The time resolution of our fast coincidence counter of $T_\mathrm{r} = 26\,\mathrm{ps}$ was about three orders of magnitude less. For incoherent illumination of the detectors the electrons behave like classical particles. Due to the insufficient time resolution a certain random coincidence rate is observed. When we change the illumination from incoherent to coherent we expect a reduction of the random coincidences (by a factor $T_\mathrm{c}/T_\mathrm{r}$ of about 10^{-3} in the present experiment) due to the fact that within the first $10^{-14}\,\mathrm{s}$ after arrival of an electron no second one is allowed to arrive. This reduction is our signature of antibunching.

1.2 Experimental set-up

Our experimental set-up corresponds to HBT's stellar interferometer: The tiny effective virtual source of an electron field emitter illuminates via magnifying quadrupoles two small collectors (Fig. 1a, right hand side, rhs). With increasing magnification the effective lateral distance of the collectors decreases and their illumination changes from incoherent

[2] While any number of photons is allowed in one cell, for electrons by Pauli's exclusion principle the occupation of a cell is one (two for antiparallel spins).

[3] The fluctuations in orthogonal polarizations resp. spin directions are independent. Therefore, when the experiment is performed with unpolarized light/electron beams, enhancement resp. suppression of the extra fluctuations is reduced by a factor 1/2 compared to polarized beams.

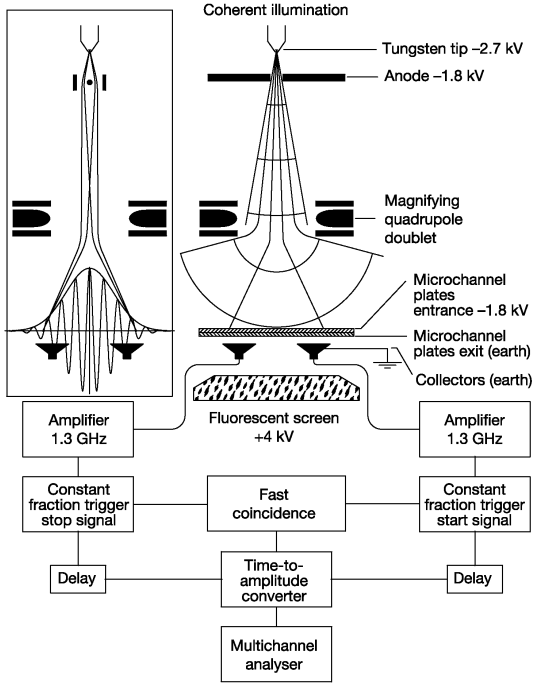

Figure 1:
Electron optical set-up (top) and fast coincidence electronics (bottom) to measure electron anticorrelations. The spherical segments emerging from the cathode represent single coherence volumina. Between the electron source and the quadrupole a biprism (inset on the left) is inserted temporarily to check the coherence of illumination of the collectors.

to totally coherent. In turn a continuous increase of anticorrelations of arrival times of the electrons is expected.

The quadrupoles produce an elliptically shaped beam of coherent electrons. For geometrical reasons less coherent electrons are missing the collectors compared to stigmatic magnification. This reduces the measuring time T_{M} largely. The collectors, 4 mm in diameter (impedance 50 Ohms) inserted between the exit of the two cascaded micro channel plates (mcp) and the fluorescent screen, collect the electron avalanches initiated by single electrons. Into the actual electron optical set-up[4] an electron biprism (inset on the left hand side, lhs, of Fig. 1) is integrated. It allows to examine the state of coherence of illumination of the collectors[5] by observing the overlap of the fringes with the shadows of the collectors on the fluorescent screen. By this means the magnification factors which are necessary for coherent, partially coherent and incoherent illumination of the collectors are determined. The antibunching

[4]Its construction principles may be found, e.g., in [12].
[5]At least in the direction perpendicular to the fringes.

experiments are performed at these predetermined magnifications without biprism in the beam path.

The very short electron avalanches leaving the channel plates (rise time and width $\sim$.5 ns) are transferred coaxially from the collectors via microwave amplifiers (bandwidth 1.5 GHz) to modified Constant Fraction Trigger (CFT) modules which extract timing signals with low time-jitter and -walk. A first coincidence circuit preselects events within a time window of ± 3 ns and opens the gate of a Time to Amplitude Converter (TAC). The time spectra are accumulated by a Multi Channel Analyzer (MCA). By an additional delay of 3 ns in the stop channel of the time to amplitude converter, arrival time zero (Fig. 2, τ=0) shows up in the center of the time spectra. Stop signals arriving prior to the start signal are displayed on the negative time axis.

The emission of electrons is a Poissonian process, therefore — for incoherent illumination — the probability of arrival of an electron after an elapsed time $\tau = t_0 - t_1$ is given by $P(\tau) = \mathrm{e}^{-\overline{n}\tau}$ where $\overline{n}$ is the average counting rate. I.e., given a start signal at time t_0, the probability for the next stop signal at t_1 depends exponentially on the counting rate $\overline{n}_{\mathrm{stop}}$ in the stop channel. In semilogarithmic representation this probability is represented by a straight line with a slope given by $-\overline{n}_{\mathrm{stop}}$ (Fig. 2, rhs).

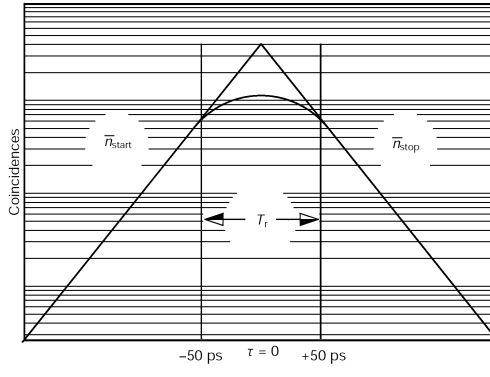

Figure 2: An example of a time spectrum expected for Poissonian processes in semilogarithmic representation, see text.

Correspondingly, stop signals arriving prior to the start signal are displayed on the negative time axis with a slope of $\overline{n}_{\mathrm{start}}$ (Fig. 2, lhs). The rounded peak corresponds to an antibunched beam at finite resolving time T_{r} of the fast coincidence. Quantitatively, the area enclosed between the straight lines and the antibunched curve below corresponds to a loss in the number of coincidences.

Features of our cold $\langle 100 \rangle$ oriented tungsten field emitter are: Extraction voltage 900 V, total current 1.5 μA, energy width ΔE_{FWHM} of .3 eV

which corresponds to a standard deviation ΔE of .13 eV (calculated under the assumption of a Gaussian energy distribution), virtual source diameter $\sim$ 36 nm, brightness $4.4 \cdot 10^7 \frac{\mathrm{A}}{\mathrm{cm}^2 \cdot \mathrm{sr}}$, coherence time $T_\mathrm{c} = 3.25 \cdot 10^{-14}$ s, coherent particle current $4.7 \cdot 10^9$ 1/s, degeneracy $1.6 \cdot 10^{-4}$.

In spite of a vacuum of 10^{-10} mbar and a constant emission current during the data accumulation times T_M (see Table 1), the counting rates of the detectors sometimes increased by more than a factor of 2 or fell below .5 of the desired value. In these cases a reduction resp. an increase in coherence of illumination of the collectors took place. Therefore, time spectra with counting rates outside these limits were discarded. $T_{\mathrm{M}_\mathrm{eff}}$ is the data accumulation time resulting after subtraction of times of unstable emission.

1.3 Results

In order to prove antibunching a total of four spectra were accumulated for about 30 hrs each. The first for incoherent illumination of the detectors, the following for partially, totally and the last again for partially coherent illumination. The evaluation procedure of the experimental time spectra consisted of smoothing and normalizing the spectra followed by visually superimposing the incoherent with the coherent resp. partially coherent spectra. The results are summarized in Fig. 3 and Table 1.

	illumination		
	part. coh.	coh.	part. coh.
$S = \Delta N$	4.567	16.942	8.292
$S_\mathrm{rel}/10^{-3}$	0.61	1.26	0.34
S/N	2.2	3.0	1.4
T_M/min	1402	1690	4531
$T_{\mathrm{M}_\mathrm{eff}}$/min	1402	1642	4450

Table 1: Summary of results. S, S_rel are the absolute, resp. relative coincidence reduction, S/N the signal-to-noise ratio, T_M the total measuring time and $T_{\mathrm{M}_\mathrm{eff}}$ the effective measuring time after subtraction of times of instable emission of the field emitter.

The antibunching signal S, i.e., the missing coincidences ΔN in the coherent and partially coherent versus the incoherent spectrum becomes

visible as a flattening of the peak in Fig. 3 within the time resolution window of ±13 ps. The measured relative reduction in coincidences amounts to $S_{\mathrm{rel}} = 1.26 \cdot 10^{-3}$ with a signal-to-noise ratio S/N of 3. As expected, the reduction in coincidence rate and the signal-to-noise ratio are smaller for partially coherent illumination. The results are in agreement with theoretical expectations [8, 13].

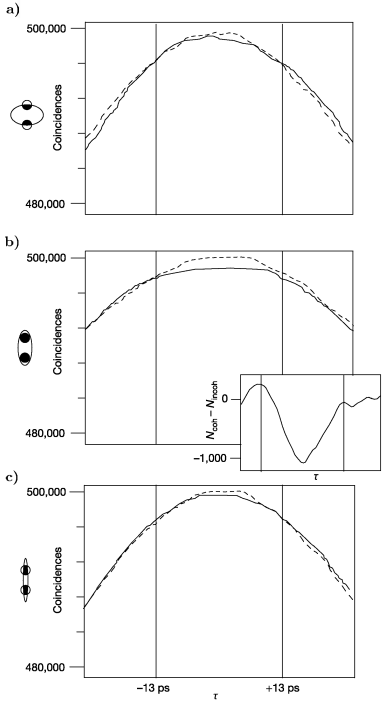

Figure 3:
Antibunching as a function of coherence of illumination of the collectors. The coincidence rate for incoherent illumination (dashed lines) is compared to that for partially coherent on top, coherent in the middle and again partially coherent illumination on the bottom (full lines). In the inset $N_{\mathrm{coh.}} - N_{\mathrm{incoh.}}$ is given. In the pictograms the ellipses represent the coherently illuminated areas, the circles the collector areas. The coherently illuminated parts of the collectors are marked in black.

1.4 Conclusion

Antibunching or — in the parlance of interferometry — interference between a system consisting of two particles resp. second order coherence has been observed for *massive free fermions*. The experimental technique opens a gateway to new fundamental tests of quantum mechanics and statistics, e.g., observation of quantum statistics on interference phenomena and experimental tests of interaction of fields and potentials with charged two-fermion systems [8].

2 Controlled decoherence in an electron interferometer

2.1 The concept of decoherence

Decoherence is the emergence of classical features of a quantum system, resulting from its — in general irreversible — interaction with the environment.

The problem of incompatibility of the quantum mechanical superposition principle with our everyday experience of a 'classical' world in which, e.g., superpositions of macroscopically distinct states are not observed and measurements give a definite result dates back to the early days of quantum mechanics. A prominent example of this apparent 'paradox' is Schrödinger's cat [14]: The decay of a single radioactive atom triggers a mechanism that sets free poison which, as a result, kills a cat. According to quantum theory, the state of the total system consisting of radioactive atom, poison apparatus, and cat should evolve into a superposition of undecayed atom, undestroyed poison ampoule and cat being alive *plus* decayed atom, destroyed poison ampoule and cat being dead. Thus, a "Schrödinger cat", as initially intended by Erwin Schrödinger, is rather an entangled state of a microscopic object (radioactive atom) with a macroscopic one (cat) than a superposition of two macroscopically distinct states (dead and alive cat) (cf. [15]). This also shows that entanglement, which is one of the main 'ingredients' of the solution — namely decoherence — of this 'paradox', is a very old concept [16, 17] and already played an important role in the 'paradox' itself. The other main 'ingredient' of the solution is the interaction with the environment. Its importance was recognized by Zeh in 1969 [18, 19]. In the following years, initially only a few authors (Zeh, Zurek, Joos, and others) worked on this topic and investigated the dynamics of systems interacting with their environment. In the last decade, the interest in decoherence has risen drastically. This fact is confirmed by the increasing number of papers (for an overview see [20, 21]).

In contrast to microscopic systems like electrons or atoms, macroscopic systems with their closely spaced energy levels unavoidably interact with their environment, e.g. with molecules of air, with photons of sunlight, and in any case with cosmic background radiation. Thereby correlations with the environment are formed — we get entanglement of the macroscopic system with its environment. Consequently, a macroscopic system can never be described by a (pure) quantum state, only the total system consisting of macroscopic object and environment is

in a well-defined quantum state. In order to come to know about the properties of the macroscopic object alone, one has to take the partial trace of the state of the total system over the unobserved environmental degrees of freedom, thereby getting a mixed state. If the states of the environment, which the different object states are entangled with, are orthogonal to each other, the resulting mixed state of the object alone is just the incoherent mixture of these object states — no interference between them is left, classical behaviour emerges.[6] Which kind of object states will become — and *stay* — entangled with *orthogonal* environment states is determined by the interaction Hamiltonian of the object with the environment [22].

The achievements of the concept of decoherence are manifold: decoherence explains why we do not observe superpositions of macroscopically distinct states or superpositions of different outcomes of a measurement, and it can explain superselection rules.

2.2 Scheme of the experiment

According to a proposal by Anglin and Zurek [23, 24], we carried out an experiment (Fig. 4) in which a highly controllable environment is realized by a resistive plate, more exactly: by the electron and phonon gas inside this plate. The object system is a free electron. So our object system is not a macroscopic system but a microscopic one, but nevertheless the interaction with this especially chosen environment — which *is* truly macroscopic — is so strong that decoherence can be observed.

The electron beam is split in two parts both of which travel over the plate at the same height, but laterally separated (see Fig. 4). An electron above a conducting plate causes an induced charge in the plate, and as the electron moves, so does the induced charge. Therefore we get

[6] In case of Schrödinger's cat paradox, it would suffice not to look at the atom in order to avoid a contradiction with what one expects from everyday experience (no superposition of dead cat plus alive cat, but also no superposition of dead cat and destroyed poison ampoule plus alive cat and undestroyed poison ampoule): Taking the trace over the states (decayed/undecayed) of the atom — which is of course a very special case of an unobserved 'environment' — gives a mixed state of the rest of the system (cat dead *or* alive according to classical expectations) in which no interference terms are left. Another possibility to solve the paradox is the existence of unobserved degrees of freedom of the cat which unambiguously indicate whether the cat is dead or alive (each of the very many states describing a cat being dead resp. alive contains a tensor product of states which are orthogonal for the cat being dead resp. alive). Also by taking the trace over one of these degrees of freedom, the classically expected result is obtained.

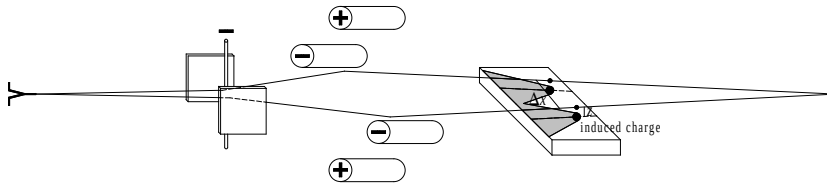

Figure 4: Sketch of the decoherence experiment. The two different trajectories of the electron over the resistive plate lead to different disturbances (shaded regions) in the electron and phonon gas inside the plate.

an electric current in the plate which encounters ohmic resistance, thus a disturbance in the electron and phonon gas inside the plate results. This disturbance is different for the two paths of the electron. So we get entanglement of the beam electron with the electron and phonon gas inside the plate. As dissipation is an irreversible process, a record of the electron's path *remains* when the electron has crossed the plate and the two parts of the beam are recombined. Therefore, the state of the combined system *beam electron and electron and phonon gas* in the primary interference plane reads

$$|\Psi\rangle = (|l\rangle|L\rangle + |r\rangle|R\rangle)/\sqrt{2}$$

where $|l\rangle$ and $|r\rangle$ are the states of the beam electron in the two different paths and $|L\rangle$ and $|R\rangle$ are the corresponding states of the electron and phonon gas. If we now measure an observable affecting only the beam electron, interference (between states $|l\rangle$ and $|r\rangle$) is the more suppressed the smaller $\langle L|R\rangle$ is. So in case of no disturbance of the plate (infinite distance z of beams to plate, or superconducting plate), contrast is maximum. But the stronger the disturbance is (decreasing height z of beams above plate) and the greater the difference between states $|L\rangle$ and $|R\rangle$ is (increasing lateral separation Δx), the less interference contrast we get.

Another way to explain the loss of contrast is to look at the "welcher Weg"(which path) information which the electron leaves in the electron gas inside the plate. The less $\langle L|R\rangle$ is, the more information is stored in the plate. As a consequence of the complementarity principle, in its particular case of wave-particle duality, interference and knowledge of the 'path' taken by the particle are mutually exclusive.

With varying height z and by varying the lateral separation Δx, the

strength of decoherence changes from negligible to full decoherence, i.e. from maximum contrast of the interference fringes to contrast zero.

Compared to other experiments on decoherence, the present one has several advantages: It realizes an actually ohmic environment (as it was supposed in the first theoretical treatments of decoherence), the quantum object is a single free elementary particle (no inner degrees of freedom are involved[7]), the interaction with the environment is due to the electric field of a charge (thus giving us an idea why the charge superselection rule is so powerful), and we get real 'pictures' of the transition from quantum to classical.

2.3 Experimental set-up

We use a compact rigid electron biprism interferometer [12]. It is distinguished by small dimensions and small mass and by the fact that all electron optical components (which are, in general, of cylindrical shape, (28 ± 0.01) mm in diameter) are tightly screwed on two high-precision ceramic rods by means of braces. Therefore, this interferometer is much less sensitive to vibrations compared to interferometers being based on electron microscopes with their large dimensions. The whole interferometer is shielded from varying magnetic fields by a tube of mu-metal. This ruggedized type of interferometer was already successfully employed, e.g., to demonstrate the Sagnac effect with electrons [25], to measure energy spectra of electrons by means of Fourier spectroscopy [26], to ensure coherence in the measurement of electron antibunching [4], and for interferometry with He^+ ions [27].

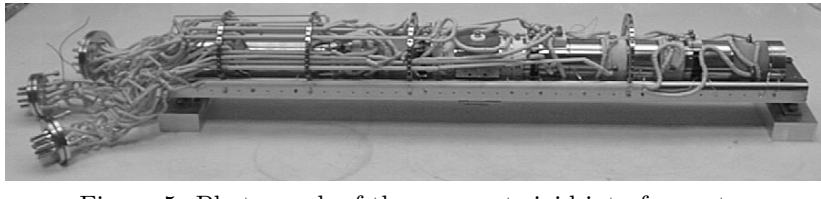

Figure 5: Photograph of the compact rigid interferometer.

As an electron source, a field emission diode system is used. Therefore, ultra-high vacuum is necessary. The electron beam is aligned to the optical axis by a double deflection element. Then the beam is split and made to diverge by a negatively charged Möllenstedt biprism [28]. The rays are directed towards each other again by an electrostatic quadrupole

[7] Due to the absence of magnetic fields, spin is irrelevant in the present experiment.

(negatively charged in the plane of the beams). Before the two beams meet, they pass the resistive plate with a lateral separation Δx. By means of vertical deflection elements (which are not shown in the figure) in front of the 'decoherence plate', the beams are made parallel to the plate. The interference pattern formed in the primary interference plane where the two beams are recombined is enlarged by electrostatic magnification quadrupoles. It is then amplified by a dual-stage channel plate image intensifier, transferred to a CCD camera by tapered fiber optics, and evaluated by an image processing system. To compensate for slight angular misalignments of the electron optical elements, coils to rotate the image are incorporated in the interferometer. As a 'decoherence plate' we use a piece of a doped silicon wafer 1 cm in length.

The resistive plate can be mechanically displaced in order to vary the height z of the beams over the plate. This is achieved by a linear feedthrough moving a wedge on which the bar with the plate glides (Fig. 6). Alternatively, the range of heights z which is mapped on the fluorescent screen (Fig. 8) can be varied using deflection elements.

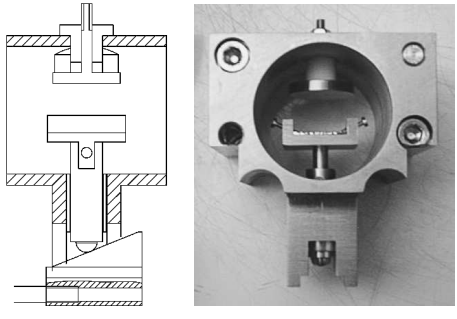

Figure 6: Element for adjusting the resistive plate in height. Side view in workshop drawing (left) and front view photograph (right).

In general, the electrostatic deflection elements will cause longitudinal shifts of the wave packets in the two beams relative to each other. Hence there will be loss of contrast also due to this effect. In order to discriminate between this and the loss of contrast ensuing from decoherence, a Wien filter (crossed-field analyzer) is included in the beam path to compensate for this longitudinal shift [29, 30]. A Wien filter consists of a crossed electric and magnetic field, both being perpendicular to the optical axis. When the matching condition $E = vB$ between electric field E and magnetic field B is fulfilled for the main velocity component v of the electron beam, the Wien filter does not cause a phase shift but only a wave packet shift. By varying the excitation of the matched

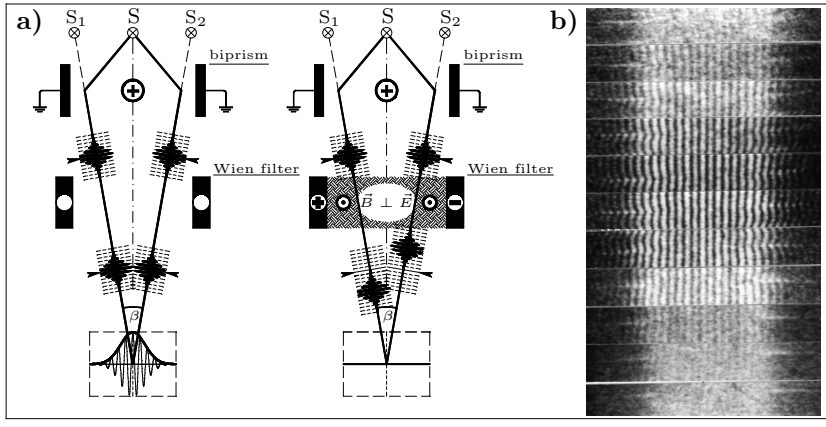

Figure 7: a) Electron biprism interferometer with Wien filter switched off (left) and Wien filter in its excited state (right): The wave packet shift exceeding the coherence length leads to the disappearance of the interference fringes. b) Restoration of contrast by a Wien filter: The longitudinal shift of the wave packets caused by electrostatic deflection elements (top) can be compensated (middle) and overcompensated (bottom) with the Wien filter [30]. The 11 micrographs correspond to 11 different excitations of the Wien filter, increasing from top to bottom.

Wien filter we can change the longitudinal distance between the interfering wave packets and thereby vary contrast (see Fig. 7). In order to get only the loss of contrast due to decoherence by the resistive plate it is indispensable to maximize contrast with the help of the Wien filter.

2.4 Results

Although the evaluation of the measurements is still in progress, we can already present qualitative results. We have clearly seen the decrease of contrast with decreasing height z of the beams over the plate (Fig. 8). These pictures are images from the quantum-classical border showing directly the transition from the quantum regime (for large z, small Δx: full interference, electron behaves as a wave) to the classical regime (for small z, large Δx: full which-path information, electron behaves as a particle with a definite trajectory). Quantitative comparison of the observed contrast with the theoretical predictions of Anglin and Zurek [23, 24] and of Levinson [31] has still to be done.

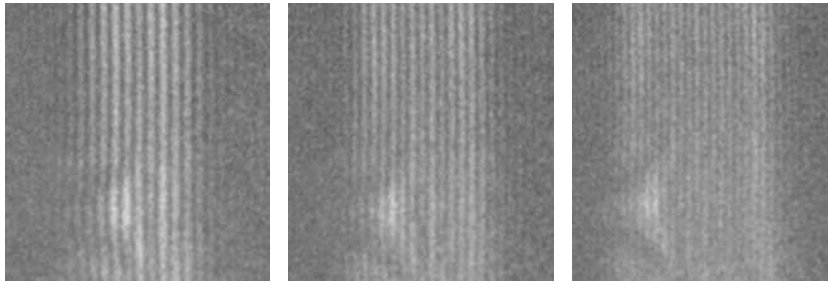

a) b) c)

Figure 8: Decoherence as a function of height z of the beams over the plate for different lateral separations Δx of the beams. The bottom of all pictures corresponds to a distance z of $\sim 10\,\mu$m from the plate, the top to $\sim 40\,\mu$m (preliminary values). The lateral separation Δx increases from a) to c). Both the increase in contrast (corresponding to a decrease in decoherence) from $z = 10\,\mu$m to $z = 40\,\mu$m and the decrease in contrast from a) to c) is clearly visible in the micrographs. The latter is caused by increasing decoherence and additionally by decreasing angular coherence with a larger lateral separation. The triangular structure is caused by charging of a dust particle on the biprism filament.

Variation of the lateral separation Δx of the beams shows that the strength of decoherence increases with increasing Δx (Fig. 8), but again, quantitative comparisons have yet to come. Besides, we are not yet able to tell if decoherence saturates [23, 24] at a certain lateral separation Δx.

Acknowledgement

We thank the Deutsche Forschungsgemeinschaft for financial support.

References

[1] R. Hanbury Brown and R.Q. Twiss, Phil. Mag. **45**, 663-682 (1954).
[2] R. Hanbury Brown and R.Q. Twiss, Nature **177**, 27-29 (1956).
[3] R.Q. Twiss and A.G. Little, Aust. J. Phys. **12**, 77-93 (1959).
[4] H. Kiesel, A. Renz, and F. Hasselbach, Nature **418**, 392-394 (2002).

[5] R. Hanbury Brown, *The Intensity Interferometer*, p. 7, New York, Taylor & Francis, 1974.
[6] E.M. Purcell, Nature **178**, 1449-1450 (1956).
[7] R. Hanbury Brown and R.Q. Twiss, Nature **178**, 1046-1048 (1956).
[8] M.P. Silverman, Phys. Lett. A **120**, 442-446 (1987) and references therein.
[9] T. Kodama et al., Phys. Rev. A **57**, 2781-2785 (1998).
[10] M. Henny et al., Science **284**, 296-298 (1999).
[11] W.D. Oliver et al., Science **284**, 299-301 (1999).
[12] F. Hasselbach, Z. Phys. B – Condensed Matter **71**, 443-449 (1988).
[13] T. Tyc, Phys. Rev. A **58**, 4967-4971 (1998).
[14] E. Schrödinger, Naturwissenschaften **23**, 807-812 (1935).
[15] W.T. Strunz, G. Alber, and F. Haake, Physik Journal **1**, 47-52 (2002).
[16] J. von Neumann, *Mathematische Grundlagen der Quantenmechanik*, Chapter VI, Berlin, Springer, 1932.
[17] E. Schrödinger, Proc. Cambridge Philos. Soc. **31**, 555-563 (1935).
[18] H.D. Zeh, Found. Phys. **1**, 69-76 (1970).
[19] K. Baumann, Z. Naturforsch. A **25**, 1954-1956 (1970).
[20] E. Joos et al., *Decoherence and the Appearance of a Classical World in Quantum Theory*, Berlin, Springer, 2003.
[21] W.H. Zurek, Rev. Mod. Phys. **75**, 715-775 (2003).
[22] W.H. Zurek, Phys. Rev. D **24**, 1516-1525 (1981).
[23] J.R. Anglin and W.H. Zurek, in *Dark Matter in Cosmology – Quantum Measurements – Experimental Gravitation : Proc. XXXIst Rencontres de Moriond*, p. 263-270, eds. R. Ansari, Y. Giraud-Héraud, and J. Trân Thanh Vân, Gif-sur-Yvette, Editions Frontieres, 1996.
[24] J.R. Anglin, J.P. Paz, and W.H. Zurek, Phys. Rev. A **55**, 4041-4053 (1997).
[25] F. Hasselbach and M. Nicklaus, Phys. Rev. A **48**, 143-151 (1993).
[26] F. Hasselbach, A. Schäfer, and H. Wachendorfer, Nucl. Instrum. Meth. A **363**, 232-238 (1995).
[27] F. Hasselbach and U. Maier, in *Quantum Coherence and Decoherence : Proc. ISQM-Tokyo '98*, p. 299-302, eds. Y.A. Ono and K. Fujikawa, Amsterdam, Elsevier, 1999.
[28] G. Möllenstedt and H. Düker, Z. Phys. **145**, 377-397 (1956).
[29] G. Möllenstedt and G. Wohland, in *Proc. Seventh Europ. Congr. Electron Microscopy*, vol. 1, p. 28-29, eds. P. Brederoo and G. Boom, Amsterdam, North Holland, 1980.
[30] M. Nicklaus and F. Hasselbach, Phys. Rev. A **48**, 152-160 (1993).
[31] Y. Levinson, J. Phys. A: Math. Gen. **37**, 3003-3017 (2004).

(Manuscrit reçu le 6 avril 2004)